Article

Abatement of Naphthalene by Persulfate Activated by Goethite and Visible LED Light at Neutral pH: Effect of Common Ions and Organic Matter

Andrés Sánchez-Yepes [ID], David Lorenzo, Patricia Sáez, Arturo Romero and Aurora Santos *[ID]

Chemical Engineering and Materials Department, Complutense University of Madrid, 28040 Madrid, Spain; andsan28@ucm.es (A.S.-Y.); dlorenzo@ucm.es (D.L.); patrisae@ucm.es (P.S.); aromeros@ucm.es (A.R.)
* Correspondence: aursan@ucm.es

Abstract: Naphthalene (NAP) has received particular attention due to its impact on the environment and human health, mandating its removal from water systems. In this work, the abatement of NAP in the aqueous phase was achieved using persulfate (PS) activated by Fe (III) and monochromatic LED light at a natural pH. The reaction was carried out in a slurry batch reactor using goethite as the Fe (III) source. The influence of the PS concentration, goethite concentration, irradiance, temperature and presence of organic matter, chloride, and bicarbonate on the abatement of NAP was studied. These variables were shown to have a different effect on NAP removal. The irradiance showed a maximum at 0.18 W·cm^{-2} where the photonic efficiency was the highest. As for the concentration of goethite and PS, the influence of the first one was negligible, whereas for PS, the best results were reached at 1.2 mM due to a self-inhibitory effect at higher concentrations. The temperature effect was also negative in the PS consumption. Regarding the effect of ions, chloride had no influence on NAP conversion but carbonates and humic acids were affected. Lastly, this treatment to remove NAP has proved to be an effective technique since minimum conversions of 0.92 at 180 min of reaction time were reached. Additionally, the toxicity of the final samples was decreased.

Keywords: goethite; LED light; naphthalene; persulfate; PAHs

1. Introduction

Rapid industrialisation and urbanisation have led to anthropogenic activities that discharge various environmental pollutants such as polycyclic aromatic hydrocarbons (PAHs) [1]. PAHs are composed of two or more fused aromatic benzene rings and due to their inherent properties, they are persistent pollutants having a wide range of biological toxicity. So, although there are more than 100 different types of PAHs, the United States Environmental Protection Agency (USEPA) has categorised 16 PAHs on the priority list due to their adverse impact on the environment and human health [2,3]. The list includes naphthalene, acenaphthylene, acenaphthene, fluorene, phenanthrene, anthracene, fluoranthene, pyrene, chrysene, benzo (a) anthracene, benzo (b) fluoranthene, benzo (k) fluoranthene, benzo (a) pyrene, indeno123-cd perylene, dibenzo (ah) anthracene, and benzo (ghi) perylene. Among these, naphthalene (NAP) is one of the most common PAHs in the environment. NAP is mainly found in moth repellents, deodorants, and cigarettes. Additionally, it is widely used in the chemical industry as a raw material for the production of dyes and pesticides, among others [4]. Unfortunately, it is reported to be a carcinogenic and mutagenic compound that has been detected in rivers, industrial effluents, and sewage wastewaters, among others [1,5,6]. It is hydrophobic, flammable, highly volatile, and chemically stable in water media and its removal from water is necessary [4]. Several technologies have been proposed for its removal, from physical technologies such as adsorption [4,7] to chemical technologies such as advanced oxidation processes (AOPs) [8] using H_2O_2 and sodium persulfate common oxidants. These oxidants must be activated to produce radical

species able to degrade rapidly persistent pollutants to increase their oxidising potential. The degradation of NAP has been studied in the literature using H_2O_2 and PS activated by iron through different methods, for example, using Fe (II) (Fenton reaction) [9,10], ultraviolet and visible light (photo-Fenton) [11], power (electro Fenton) [12], and persulfate activated by iron [13–15] or by using both oxidants [16]. Despite the removal of NAP reported in those works often reaching 90%, there are several drawbacks, such as the need to operate at an acidic pH and the generation of iron in the solution, which must be removed in additional treatments (for example, neutralisation, separation, and management of the iron hydroxide sludge generated). These drawbacks can be overcome if a stable solid catalyst is used. This catalyst has to be cheap, environmentally friendly, easily separable from the solution, and with depictable leaching of the active phase (iron) [17]. Naturally occurring iron minerals, whose main characteristics are abundance and affordability, have been studied in the heterogenous process, including hematite, pyrite, goethite, and magnetite, which have been successfully applied in AOPs [18]. Heterogeneous Fenton has been applied in NAP removal with success without light [14] using siderite as the catalyst and with visible light [11]. However, the visible light used was source Hg or Xe lamps, which need complicated cooling and are toxic. For this reason, commercial visible light-emitting diode lamps (VIS LED) have been recently proposed as an innovative light source for the removal of organic pollutants from water at a neutral pH using natural iron minerals and hydrogen peroxide as the oxidant [19]. However, the efficiency of H_2O_2 decreased in the presence of high carbonate contents in water due to non-productive reactions [20–23], and the use of PS is recently gaining attention. PS shows high aqueous solubility, high stability, is relatively inexpensive, and generates benign end products [24–27]. It can be activated with a transition metal complex, using light or heat, adding hydroxide peroxide, or using an alkali (pH > 10) [23,28–30] producing sulfate radicals. Sulfate radicals are strong oxidants, less selective, and more stable on a broader pH interval than hydroxyl radicals.

This work aims to remove NAP in the aqueous phase using PS activated by VIS LED as a light source and goethite as a heterogeneous catalyst. To our knowledge, this system has not been previously studied. The influence of different variables has been addressed, such as PS and catalyst concentrations, the irradiance of the light source used, and the temperature and presence of other ions and natural organic matter in the solution. In addition, the toxicity of the water obtained after the treatment has been studied.

2. Results and Discussion

The conversion of NAP and PS obtained in runs summarised in Table 1 has been calculated with the reaction time by Equation (1) and Equation (2), respectively.

$$X_{\text{NAP}} = 1 - \frac{C_{\text{NAP}}}{C_{\text{NAP},0}} \tag{1}$$

$$X_{\text{PS}} = 1 - \frac{C_{\text{PS}}}{C_{\text{PS},0}} \tag{2}$$

X_{NAP} *and* X_{PS} are the NAP and PS conversions, respectively; C_{NAP} *and* C_{PS} are the NAP and PS concentrations at a reaction time *t*, respectively; and $C_{\text{NAP},0}$ *and* $C_{\text{PS},0}$ are the naphthalene and persulfate initial concentrations, respectively.

Blank runs B1, B2, and B3 in Table 1 give NAP conversion lower than 10% at 180 min.

The complete profile of NAP and PS concentrations with time has been studied in R1 (Table 1) using $C_{\text{NAP},0} = 0.1$ mM, $C_{\text{PS},0} = 1.2$ mM, $I = 0.18$ W·cm^{-2}, and $C_{\text{GOE}} = 0.1$ g·L^{-1} and 25 °C. The reaction was carried out for a total time of 360 min. The measured NAP and PS conversions with reaction times in R1 are shown in Figure S2 of the Supplementary Materials. As shown in Figure S2, the conversion of NAP was 0.79 in the first 60 min. After this time, depletion of this conversion was observed, reaching a conversion of 0.96 at 180 min. After this time, the conversion was kept almost constant until 360 min. The same trend was observed in the PS conversion.

The PS consumption was 0.086 in the first hour, then increased to 0.19 at 180 min and remained constant during the next 180 min. For these reasons, runs R2 to R9 and S1 to S3 were maintained for 180 min. In these runs, samples were taken at 30 min and 180 min to study the effects of the variables on NAP oxidation.

Table 1. Experimental conditions of experiments. Initial NAP concentration 0.1 mM.

Experiment	T (°C)	C_{PS} (mM)	C_{GOE} ($g \cdot L^{-1}$)	I ($W \cdot cm^{-2}$)	C_{Cl^-} (ppm)	C_{HCO3^-} (ppm)	$C_{H.Ac}$ (ppm)	t (min)
B1	25	1.2	0	0.24	0	0	0	180
B2	25	0	0.1	0.24	0	0	0	180
B3	25	1.2	0.1	0	0	0	0	180
R1	25	1.2	0.1	0.18	0	0	0	360
R2	25	1.2	0.1	0.1	0	0	0	180
R3	25	1.2	0.1	0.18	0	0	0	180
R4	25	1.2	0.1	0.24	0	0	0	180
R5	25	1.2	0.2	0.18	0	0	0	180
R6	25	0.6	0.1	0.18	0	0	0	180
R7	25	2.4	0.1	0.18	0	0	0	180
R8	25	4.8	0.1	0.18	0	0	0	180
R9	40	1.2	0.1	0.18	0	0	0	180
S1	25	1.2	0.1	0.18	500	0	0	180
S2	25	1.2	0.1	0.18	0	600	0	180
S3	25	1.2	0.1	0.18	0	0	50	180

2.1. Effect of Irradiance

The influence of the absolute irradiance in NAP reduction was evaluated by varying the nominal power of the LED light source irradiated over the reactor window.

Figure 1a,b show the NAP and PS conversions, respectively, obtained at 30 and 180 min in runs B3, R2, R3, and R4, carried out at several irradiances (within the range 0 to 0.24 W·cm^{-2}). As can be seen, run B3 was carried out in the absence of LED light, and the NAP conversion was close to 0.10 at 180 min. This conversion could be explained by the loss of NAP from the medium by evaporation or adsorption [13]. At the same time, the production of sulfate radicals was not observed since no PS conversion was experimentally obtained in the absence of LED light. On the contrary, the LED light enhances the reduction of Fe (III) to Fe (II), promoting PS activation and sulfate radical production, as indicated in Equations (3) and (4)

$$Fe(III) - goethite \xrightarrow{light} Fe(II) - goethite \tag{3}$$

$$Fe(II) - goethite + S_2O_8^{2-} \rightarrow Fe(III) - goethite + SO_4^{-2} + SO_4^- \cdot \tag{4}$$
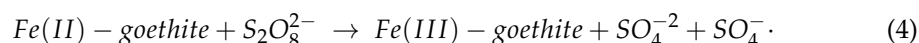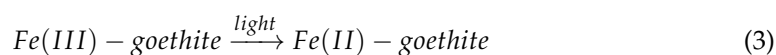
When the GOE surface is irradiated (runs R2, R3, and R4) with the monochromatic LED, sulfate radicals are produced and oxidise NAP. As shown in Figure 1, the higher the irradiance, the higher the NAP and PS conversions after 30 min of reaction time. However, the difference between the NAP conversion values using irradiance of 0.18 and 0.24 W·cm^{-2} was lower than 5%. This fact has been explained in the literature, considering that the number of photons that can trigger more electron holes on the GOE surface increases with the lamp irradiance until a specific irradiance value. Above that value, the effect of lamp irradiance on the pollutant conversion is insignificant [19,31]. Under experimental conditions in R2, R3, and R4, an almost total conversion of NAP was achieved at 180 min.
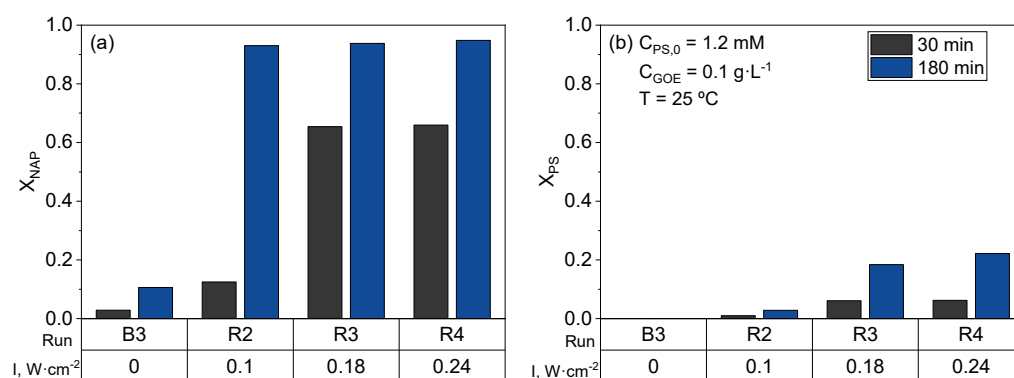
Figure 1. Effect of irradiance in (**a**) conversion of NAP; (**b**) conversion of PS at 30 min and 180 min. $C_{NAP,0} = 0.1$ mM, $C_{PS,0} = 1.2$ mM, $C_{GOE} = 0.1$ g·L^{-1} and 25 °C.

In Table S1, the initial and final pHs measured at the end of the reactions (180 min) are summarised. As shown in Table S1, final pHs are close to 3, except for B3 which has a final pH of 5.44. The acidification of the reaction media can be attributed to PS decomposition and the formation of acid intermediates during naphthalene oxidation.

The photodegradation of NAP under different operating conditions of irradiance was analysed using the photonic efficiency η_p $\left(\text{mol}_{NAP} \cdot \text{Einstein}^{-1} \right)$ defined in Equation (5). This photonic efficiency is the ratio between the number of moles of pollutant converted and the number of photons reaching the reactor window over a defined range of wavelengths (350–600 nm).

$$\eta_p = \frac{C_{NAP,0} \cdot X_{NAP} \cdot V_R}{F_E \cdot \left(t_f - t_0 \right)} \tag{5}$$

where $C_{NAP,0}$ is the initial concentration of NAP (mol·L^{-1}) and X_{NAP} is the conversion of NAP achieved at the time t_f (30 min of reaction). V_R refers to the reactor volume (0.1 L) and F_E is the flow of photons (Einstein s^{-1}) irradiated over the reactor window.

The photon flow that reached the reactor window can be estimated by applying Equation (6) measuring the absolute irradiance (I_a) in three different positions of the reactor window.

$$F_E = \int_0^A \int_{\lambda_0}^{\lambda_f} \frac{I_a}{h \cdot \frac{c}{\lambda}} \cdot d\lambda \cdot dA \tag{6}$$

I_a is the average of absolute irradiance measured with the spectrometer coupled with an optical fibre and a cosine corrector in W·cm^{-2}·nm^{-1}; λ is the wavelength, and h and c are the Plank constant at light speed, respectively. A is the total evaluated area of the reactor window (cm^2).

The photon flow was calculated from the average values of absolute irradiance in Figure S3 and integrating Equation (6). In Table 2, the photonic efficiencies are summarised. These values were calculated using the experimental results of the NAP conversion after 30 min at different irradiance values (Figure 1).

Table 2. Photonic efficiencies at different ca irradiances, calculated from the experimental values of NAP conversion in Figure 1 and the photons flow irradiated over the reactor window.

I $\left(\text{W·cm}^{-2} \right)$	0.1	0.18	0.24
η_p $\left(\text{mol}_{NAP} \cdot \text{Einstein}^{-1} \right)$	1.82×10^{-4}	5.36×10^{-4}	4.03×10^{-4}

As can be seen in Table 2, the η_p presented a maximum value when the reactor was irradiated with $I = 0.18$ W·cm^{-2}. This value inferred the use of a higher irradiance value performing an unnecessary waste of photon flow that was not used to activate the PS in

the NAP abatement. On the other hand, irradiance values lower than $0.18 \text{ W} \cdot \text{cm}^{-2}$ were not considered since the photonic efficiency decreased, meaning lower NAP oxidation.

2.2. Effect of Goethite Concentration

The decrease of NAP was studied in the absence of the catalyst and using 0.1 and $0.2 \text{ g} \cdot \text{L}^{-1}$ of GOE with 1.2 mM of PS and $0.18 \text{ W} \cdot \text{cm}^{-2}$ of lamp irradiance. The conversion of NAP obtained and the PS consumption are plotted in Figure 2. As can be seen, significant NAP conversion is only noticed when the catalyst is added to the reaction medium. The wavelength used (470 nm) was selected attending to the optical properties of GOE [19], promoting the reduction of Fe (III) in the GOE surface to Fe (II) (Equation (3)), and yielding sulfate radicals (Equation (4)) that caused the NAP oxidation.
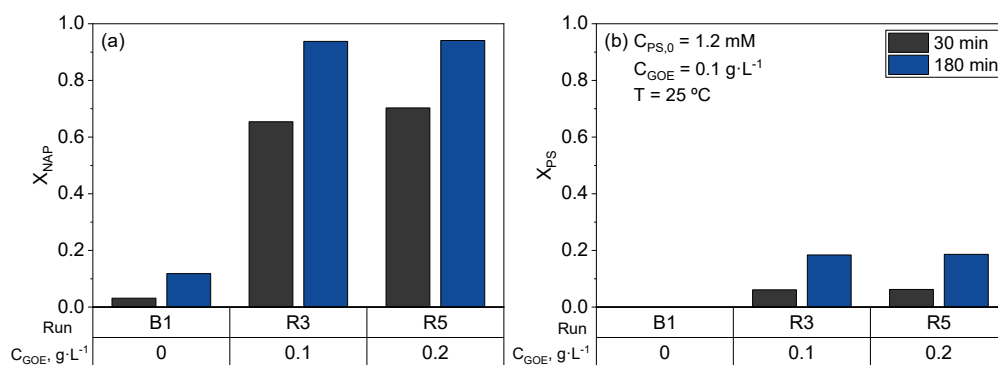
Figure 2. Effect of goethite concentration in (**a**) conversion of NAP; (**b**) conversion of PS at 30 min and 180 min. $C_{NAP,0} = 0.1 \text{ mM}$, $C_{PS,0} = 1.2 \text{ mM}$, $I = 0.18 \text{ W} \cdot \text{cm}^{-2}$ and 25 °C.

As shown in Figure 2a, negligible differences in the conversion of NAP and PS were found in the GOE concentration range from 0.10 to $0.20 \text{ g} \cdot \text{L}^{-1}$ at 30 min of reaction time and using the same irradiance and initial oxidant concentration. This low difference of conversions observed in runs R3 and R5 was in agreement with that observed in a previous work where the increase in the catalyst concentration did not increase the reaction rate [32]. The minor differences observed using a twofold catalyst concentration can be attributed to the reaction taking place on the catalyst surface. In a well-mixed slurry reactor, the solid can form agglomerates reducing the active surface area of the catalyst. The latter affected the conversions of NAP and PS in two ways, promoting (i) a defective liquid–solid contact, meaning a lower contact between PS and the active sites and (ii) the scattering-out of the light, yielding a decrease in the irradiated area of the catalyst reducing the reaction of Fe (III) to Fe (II) [32].

The iron leaching from the solid catalyst to the aqueous phase was studied, measuring the total iron in the solution at 180 min of reaction time by atomic emission spectroscopy. The iron concentration in all runs was lower than $0.03 \text{ mg} \cdot \text{L}^{-1}$. The low content of Fe in the aqueous phase proves that the reaction occurs only on the solid catalyst surface.

Regarding the pH, except for B1 ($pH_f = 5.01$), the final pH values reached were 3.20 (Table S1), with a similar conversion of PS at 180 min in R3 and R5

2.3. Effect of Temperature

The decrease of NAP was investigated under two different temperatures 25 °C and 40 °C. The NAP and PS conversions obtained at the same initial concentrations of NAP, PS, and irradiance are summarised in Figure 3. As shown, the temperature slightly enhanced the reduction of NAP at 30 min, with a NAP conversion of 0.65 at 25 °C and 0.75 at 40 °C. However, after 180 min of reaction time, the NAP conversion obtained at both temperatures reached similar values (close to unity). However, the consumption of PS was higher at 40 °C than at 25 °C at 30 min and 180 min (Figure 3b).
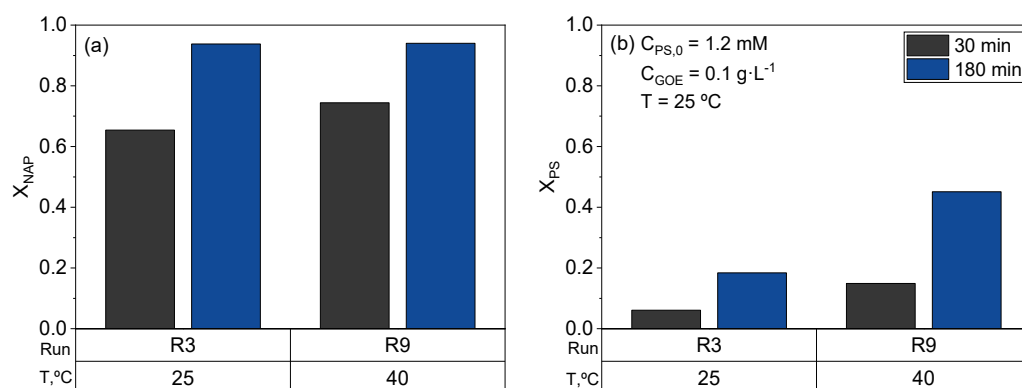
Figure 3. Effect of temperature in (**a**) conversion of NAP; (**b**) conversion of PS at 30 min and 180 min. $C_{\text{NAP},0} = 0.1$ mM, $C_{\text{PS},0} = 1.2$ mM, $I = 0.18$ W·cm^{-2} and $C_{\text{GOE}} = 0.1$ g·L^{-1}.

At 40 °C, PS activation by temperature can be performed, generating more sulfate radicals than those obtained at 25 °C [33]. This fact can be experimentally observed since the higher the temperature, the higher the conversion of PS and NAP [34,35].

2.4. Effect of PS Concentration

The oxidant concentration was tested within 0–4.8 mM using the same GOE concentration and irradiance values. The obtained conversions of NAP and PS are summarised in Figure 4. As shown in Figure 4, negligible NAP oxidation occurred without PS (B2). In runs R6 and R3, using 0.6 mM and 1.2 mM PS concentrations, a similar conversion of NAP was obtained after 30 min of reaction. On the other hand, an initial concentration of PS higher than 2.4 mM resulted in slightly lower values of NAP conversion at 30 min. The observed effect of the higher PS concentration and the lower NAP conversion can be explained by the reactions in Equations (7) and (8). This phenomenon was in agreement with Zeng [13] et al. and Kusic et al. [36]. They concluded that the production of $SO_4^- \bullet$ increases with the increase in PS. The radical sulfate in high concentrations reacts with the PS (Equation (7)), resulting in the unproductive reaction of the oxidant. In addition, $SO_4^-\bullet$ in high concentrations can be self-consumed in a self-inhibitory reaction (Equation (8)); therefore, the $SO_4^-\bullet$ available to abate the NAP decreased [13,36].

$$S_2O_8^{2-} + SO_4^- \bullet \rightarrow S_2O_8^- \bullet + SO_4^{2-} \tag{7}$$

$$2\,SO_4^- \bullet \rightarrow S_2O_8^{-2} \tag{8}$$

The NAP conversion achieved at 180 min was similar at all PS concentrations, close to unity.

2.5. Ions and Organic Matter Effects

The effects of different ions (Cl^- and HCO_3^-) and organic matter (humic acid (HuAc)) found in natural waters on the NAP conversion have been studied, comparing the NAP degradation in the presence and absence of these compounds in the aqueous phase. The experimental values of NAP and PS conversions in runs S1, S2, and S3 are summarised in Figure 5 and compared with the results obtained in R3.

All reactions in Figure 5 were carried out under the same initial PS and NAP concentrations and irradiance conditions. As shown in Figure 5a, the degradation of NAP was slightly reduced in the presence of chloride ions, indicating that this specie does not exert a remarkable effect on NAP conversion. However, a significant decrease in NAP conversion was found when bicarbonate or humic acid were added to the reaction media.
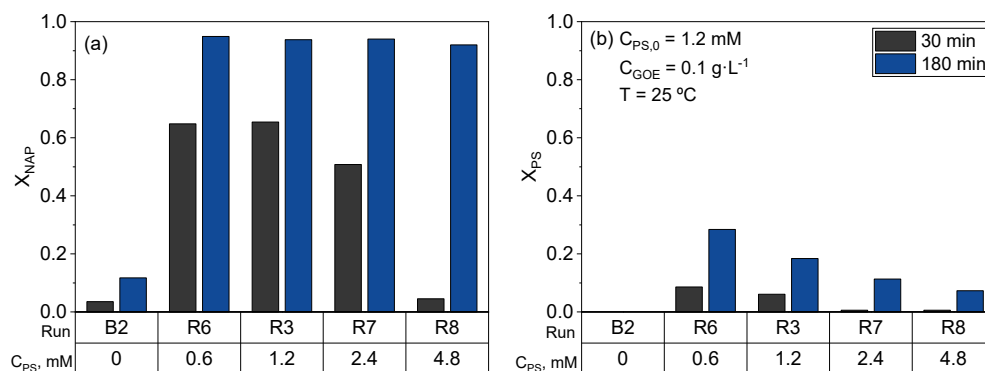
Figure 4. Effect of PS concentration in (**a**) conversion of the NAP; (**b**) conversion of PS at 30 min and 180 min. $C_{NAP,0} = 0.1$ mM, $I = 0.18$ W·cm^{-2}, $C_{GOE} = 0.1$ g·L^{-1}·cm^2 and 25 °C.
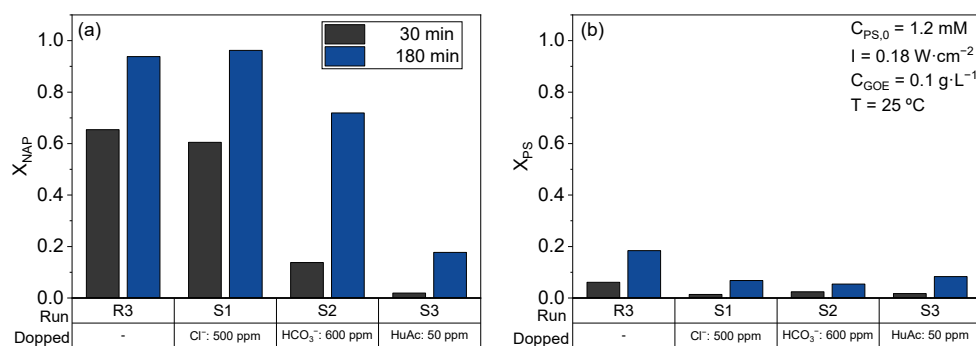
Figure 5. Effect of ions and organic matter in (**a**) Conversion of the NAP; (**b**) Conversion PS at 30 min and 180 min. $C_{NAP,0} = 0.1$ mM, $I = 0.18$ W·cm^{-2}, $C_{GOE} = 0.1$ g·L^{-1}·cm^2, $C_{PS,0} = 1.2$ mM, $pH_0 = 7$ and 25 °C.

In the presence of a high bicarbonate concentration (run S2), NAP conversion at 30 min was one-third of the value obtained without bicarbonate (R3). The scavenger effect of sulfate radicals by bicarbonate ions has been already reported in the literature [24] and results in the production of $HCO_3\bullet$ (Equation (9)) or $CO_3^-\bullet$ (Equation (10)) radicals.

$$CO_3H^- + SO_4^-\cdot \rightarrow SO_4^{2-} + HCO_3\cdot \qquad (9)$$

$$CO_3^{2-} + SO_4^-\cdot \rightarrow SO_4^{2-} + CO_3^-\cdot \qquad (10)$$
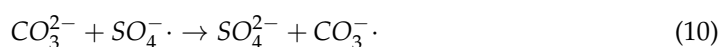
The redox potential of carbonate and bicarbonate radicals (1.63 V) is much lower than the redox potential of sulfate radicals (2.70 V) [37], explaining the inhibitory effect of bicarbonate on NAP conversion.

The effect of the presence of natural organic matter in the reaction medium was studied using 50 mg·L^{-1} of humic acid (HuAC) (Run S3). As shown in Figure 5a, a remarkable decrease in NAP conversion was obtained in the presence of HuAc at 30 min. At 180 min, NAP conversion was reduced by about 50% to that obtained in the absence of HuAc (Run R3). The inhibitory effect of HuAc on NAP conversion was even more remarkable than that noticed with bicarbonate. These findings can be explained by turbidity and the colour of the solution obtained with the solubilisation of HuAC. The appearance of the reaction medium in the runs carried out in the presence (run S3) and absence of HuAc (run R3) are shown in Figure S4 of the Supplementary Materials. As shown in Figure S4a, before the lamp is switched on, the reaction mixture of run S3 showed an intense colouration compared to the appearance of the reaction medium without HuAC Figure S4c (run R3). The intense colouration associated with HuAC in the reaction medium can modify the light capable of activating the goethite, thus decreasing the NAP conversion. Despite the

intense colouration observed in the presence of HuAC, a remarkable conversion of NAP was obtained at 180 min (50%). The colouration of natural water is scarcely as intense as that obtained in run S3, and the inhibition expected in these natural waters will be lower than that found in S3.

2.6. Toxicity Analysis

Toxicity tests were performed using a standard process (Microtox®) to monitor the bacterium Photobacterium phosphoreum. The toxicity of the reaction samples after 180 min was measured at 15 min and 15 °C, expressed as toxicity units (*TU*). *TU* was used as a direct measurement of the acute toxicity and it was calculated from the IC_{50} values at 15 min and 15 °C, applying Equation (11). The *TU* obtained from the untreated aqueous solution of 0.1 mM in NAP was also measured giving a value of *TU* = 1.76. This value is considered the reference value, TU_o. For each reaction, the *TU* of the aqueous sample at the final time (t = 180 min) was measured and the ratio *TU* to TU_o has been calculated. The corresponding results are summarised in Table 3.

$$TU = \frac{100}{IC_{50}} \tag{11}$$

TU/TU_o ratios lower than unity indicate that the toxicity of the reaction mixture was reduced after the oxidation treatment. As seen in Table 3, the higher the lamp irradiance (runs R2, R3, R4), the lower the toxicity of the reaction media. Only the lower irradiance used (run R2) increases the initial toxicity. On the contrary, *TU*s obtained in runs R3 and R4 are lower than the initial value. The GOE concentration does influence the toxicity obtained at 180 min, but the final toxicity is always lower than the initial one.

The PS concentration has a remarkable effect on the final toxicity of the reaction media, as seen in Table 3. The higher the PS concentration, the higher the reduction of the initial toxicity. At the lowest PS concentration (0.6 mM), the toxicity of the reaction media at 180 min is higher than the initial one. On the contrary, at a PS concentration above 1.2 mM, the final toxicity at 180 min is lower than the initial value. At the highest PS concentration (4.8 mM), a reduction of 85% of the initial toxicity was found at 180 min.

The differences in *TU*s obtained at 180 min can be explained by the byproducts produced and reacted during NAP oxidation. In most of the runs seen in Table 3, the NAP conversion at 180 min was close to unity. Unfortunately, no organic intermediates were significantly identified by ionic chromatography, GC/MS chromatography, or HPLC. Only traces of DEHP (Di (2-ethylhexyl) phthlate) were detected in some runs, agreeing with what was reported in the literature. However, the toxicity decrease found at 180 min ensures that non-toxic intermediates remain in the reaction media. The toxicity is remarkably reduced using a sufficient PS concentration, confirming the treatment benefits.

Lastly, the effect of temperature on *TU*s was studied. As can be seen in Table 3, an increase in the temperature does not produce a reduction in the initial toxicity. This can be explained as a higher unproductive consumption of PS occurs when the temperature increases. PS is not reacting with the byproducts but with an unproductive consumption of PS.

Table 3. Ratio of *TU* of the reaction samples after 180 min to initial Toxicity (*TU*o = 1.76).

Experiment	*T* (°C)	C_{PS} (mM)	C_{GOE} (g·L^{-1})	*I* (W·cm^{-2})	*TU/TU$_o$* 15 min
NAP					1.00
			Effect of irradiance		
R2	25	1.2	0.1	0.10	1.54
R3	25	1.2	0.1	0.18	0.79
R4	25	1.2	0.1	0.24	0.62
			Effect of goethite concentration		
R3	25	1.2	0.1	0.18	0.79
R5	25	1.2	0.2	0.18	0.79
			Effect of PS concentration		
R6	25	0.6	0.1	0.18	1.36
R3	25	1.2	0.1	0.18	0.79
R7	25	2.4	0.1	0.18	0.36
R8	25	4.8	0.1	0.18	0.14
			Effect of temperature		
R3	25	1.2	0.1	0.18	0.79
R9	40	1.2	0.1	0.18	1.06

3. Material and Methods

3.1. Chemicals

Naphthalene (NAP, $C_{10}H_8$) of analytical quality was purchased from Sigma-Aldrich (Darmstadt, Germany). This compound was dissolved in methanol (Fisher-Chemical, Hampton, CV, USA) to prepare the standards used in the calibration curve.

Sodium persulfate (PS, $Na_2S_2O_8$), used as oxidant, and Goethite (GOE), used as catalyst, were supplied by Sigma-Aldrich (Darmstadt, Germany). GOE is composed of 57.3 wt. % Fe (III) with a specific surface area (S_{BET}) of 10.24 m^2·g^{-1} [32]. Potassium iodide (KI, Fisher-Chemical, Hampton, CV, USA) and sodium hydrogen carbonate ($NaHCO_3$, Panreac, Darmstadt, Germany) were used for PS quantification. The latter was also used for the ions studied along with sodium chloride (NaCl), supplied by Sigma Aldrich (Darmstadt, Germany). Humic acid (H.Ac) 45–70% (Acros Organics, Hampton, CV, USA) was used to analyse the influence of organic matter in the aqueous media. All the reagents employed were of analytical grade. Solutions were prepared with ultra-pure water produced by a deionising system (Millipore Direct-Q).

3.2. Experimental Setup

The experiments were carried out in a cylindrical batch reactor made of borosilicate glass with an operating volume of 100 mL. The reaction mixture was agitated using a magnetic plate (IKA C-MG HS 7, Staufen, Germany) to remove the mass transfer limitations. For temperature control of the reactor, an outer jacket coupled to a pumped water bath was used. The temperature was controlled using a PID controller. The reaction medium was illuminated with a monochromatic LED lamp (470 nm) located at the top of the reactor. The distance between the lamp and the reaction surface was 11 cm. The light emitter was located at the focal plane of a collimating lens with a clear aperture of 1 cm (pre-adjusted in the factory). The collimator light sources produce an optical power output of up to 4.17 W. The power can be adjusted using a Mightex BLS-13000-1E LED controller. The output current (0–13 A) can be controlled manually. The light LED source emits over

a surface reaction of 11 cm^2, coincident with the reactor window. Figure S1 shows the experimental setup.

3.3. Experimental Procedure

Three sets of experiments were carried out to study the removal of NAP. The first one corresponds to blank runs carried out in the absence of oxidant, catalyst, or light (B1–B3). The second set studies the influence of variables such as temperature, PS concentration, and irradiance (R1–R9). The third set studies the effect of commons ions and natural organic matter in natural water on NAP conversion (S1–S3). The experimental conditions of the runs carried out are summarised in Table 1.

The experiments were carried out by dissolving NAP in water at 25 °C to achieve a concentration of 0.1 mM. This solution of 0.1 mM was used to charge the reactor with the corresponding mass of the catalyst to obtain GOE concentrations ranging from 0.1 g·L^{-1} to 0.2 g·L^{-1}. A volume of a concentrated PS solution (400 mM) was added to obtain a final PS concentration in the reaction media ranging from 0.6 mM to 4.8 mM. Once the goethite presented a good suspension (keeping an agitation of 500 r.p.m), the LED light was turned on (zero time). All the experiments were carried out at natural pH.

Reaction samples were analysed at different times. An amount of 2 mL of the reaction media was withdrawn and the goethite was separated from the aqueous phase using a nylon filter (0.22 μm). NAP concentration was analysed in the filtrate by HPLC, and the remaining PS concentration was determined by iodometric titration. At the end of the reaction (180 min), the toxicity of the samples was measured by the Microtox® bioassay. Runs were carried out in triplicate, with the standard deviation lower than 5% in all cases.

3.4. Analytical Methods

The aqueous NAP concentration was analysed using high-performance liquid chromatography (Agilent 1100 Series) equipped with a UV detector. A Poroshell 120 SB-C18 2.7 μm (4.6 × 100 mm) column was used. The mobile phase used was methanol–water (80:20, *v/v*) at a flow rate of 0.5 mL·min^{-1} and the effluent was monitored at 254 nm. This method is similar to that in the literature for NAP quantification [13,15].

The PS concentration changes with the reaction times were determined by iodometric titration using a potentiometric titration analyser (Metrohm, Tiamo 2.3, Gallen, Switzerland).

The LED lamp irradiance and intensity were measured with a Flame UV-VIS spectrometer in the 200–850 nm wavelength range coupled to a monacolin UV-Visible optical fibre of 100 μm core diameter using a cosine corrector (Ocean Insight, Duiven, The Netherlands). The spectrometer and fibre were radiometrically calibrated using the cosine corrector (CC-3) with an HL-3P-CAL lamp (Ocean Insight, Duiven, The Netherlands).

The acute toxicity of the liquid samples at the final reaction time was determined by a standard bioassay following the Microtox test procedure (ISO 11348-3, 2009) using a Microtox® M500 analyser (Azur Environmental). This test is based on bioluminescence inhibition of the bacteria *Vibrio Fischeri* when exposed to a toxicant. The method was performed at 15 °C and 15 min of exposure. The samples were fixed at pH 6–7 and persulfate neutralised with sodium thiosulfate to carry out the experiments. Phenol was used as a reference toxicant, and a test was conducted in each set of experiments to ensure that comparisons between the two sets of experiments could be made. The pH was analysed in all experiments with a Metrohm 914 pH/conductometer.

4. Conclusions

From the results obtained, it can be inferred that activation of persulfate by goethite intensified by VIS-LED light is effective on the oxidation of naphthalene in an aqueous solution. This system allowed working at an initial neutral pH at room temperature and with the iron source in a solid phase, overcoming several of the barriers of the traditional Fenton and photo-Fenton processes.

This method found that the conversion of naphthalene reached was 0.94 in only 180 min of reaction time at room temperature when 1.2 mM of oxidant is employed independently of the irradiance and catalyst concentration.

Regarding the effect of ions and organic matter, a strong influence on the oxidation of NAP when there are HCO_3^- ions and humic acid in the aqueous media was observed. This influence is because part of the PS is lost in attacking these species or generating radicals with lower oxidising power. In addition, an increase in the turbidity and colour was noted with HuAc, which may hinder the photon flux.

Additionally, the toxicity units of the aqueous phase after treatment were determined using the Microtox® technique to determine if the NAP oxidation byproducts are more toxic than naphthalene. The results showed that the final toxicity was notably reduced when the PS concentration increased. More slight or null effects of lamp irradiation and goethite concentration, respectively, were noticed on the final TUs, and the negative effect of temperature on the TUs was noticed. Only at the lowest lamp irradiance or the lowest PS concentration employed was an increase in the initial toxicity measured. A total NAP conversion and a reduction of 85% of the initial toxicity were achieved at 4.8 mM of PS, indicating the effectivity of the treatment applied.

The technique proposed in this manuscript has been demonstrated to be effective for the removal of NAP, achieving in most cases a conversion of 0.92 at 180 min. Future research should be directed towards the use of real water polluted with naphthalene based on the knowledge obtained from the study of the variables.

Supplementary Materials: The following are available online at https://www.mdpi.com/article/10.3390/catal12070732/s1, Figure S1. Schematic representation of the experimental setup; Table S1. Initial and end pH of the different experiments summarized in Table 1; Figure S2 Temporal evolution of NAP and PS conversion, (R1). Determination of reaction time and study. Maintaining $C_{NAP,0} = 0.1$ mM, $C_{PS,0} = 1.2$ mM, $I = 0.18$ W·cm^{-2}, $C_{GOE} = 0.1$ g·L^{-1} and 25 °C; Figure S3. Discretized spectral irradiance measured at the reactor window for different lamp nominal powers (Pn); Figure S4 Images of the physical appearance of the reactor medium corresponding to run S3 $C_{NAP,0} = 0.1$ mM, $C_{PS,0} = 1.2$ mM, $I = 0.18$ W·cm^{-2}, $C_{H.Ac} = 50$ *ppm* and $C_{GOE} = 0.1$ g·L^{-1}. (a) Medium without illumination (b) Medium illuminated by LED lamp. Images of the physical appearance of the reactor medium corresponding to run R3 $C_{NAP,0} = 0.1$ mM, $C_{PS,0} = 1.2$ mM, $I = 0.18$ W·cm^{-2} and $C_{GOE} = 0.1$ g·L^{-1}. (c) Medium without illumination (d) Medium illuminated by LED lamp.

Author Contributions: Conceptualization, D.L. and A.S.-Y.; methodology, D.L.; software, P.S.; validation, D.L. and A.S.; formal analysis, A.S.; investigation, P.S. and A.S.-Y.; resources, A.S. and A.R.; data curation, P.S. and A.S.-Y.; writing—original draft preparation, P.S. and A.S.-Y.; writing—review and editing, D.L.; supervision, A.S. and D.L.; project administration, A.S. and A.R.; funding acquisition, A.S. and A.R. All authors have read and agreed to the published version of the manuscript.

Conflicts of Interest: The authors declare no conflict of interest.

References

1. Mojiri, A.; Zhou, J.L.; Ohashi, A.; Ozaki, N.; Kindaichi, T. Comprehensive review of polycyclic aromatic hydrocarbons in water sources, their effects and treatments. *Sci. Total Environ.* **2019**, *696*, 133971. [CrossRef] [PubMed]
2. Patel, A.B.; Shaikh, S.; Jain, K.R.; Desai, C.; Madamwar, D. Polycyclic Aromatic Hydrocarbons: Sources, Toxicity, and Remediation Approaches. *Front Microbiol.* **2020**, *11*, 562813. [CrossRef] [PubMed]
3. Wise, S.A.; Sander, L.C.; Schantz, M.M. Analytical Methods for Determination of Polycyclic Aromatic Hydrocarbons (PAHs)—A Historical Perspective on the 16 U.S. EPA Priority Pollutant PAHs. *Polycycl. Aromat. Compd.* **2015**, *35*, 187–247. [CrossRef]
4. Alshabib, M. Removal of naphthalene from wastewaters by adsorption: A review of recent studies. *Int. J. Environ. Sci. Technol.* **2021**, *19*, 4555–4586. [CrossRef]
5. Sarria-Villa, R.; Ocampo-Duque, W.; Paez, M.; Schuhmacher, M. Presence of PAHs in water and sediments of the Colombian Cauca River during heavy rain episodes, and implications for risk assessment. *Sci. Total Environ.* **2016**, *540*, 455–465. [CrossRef]

6.   Froehner, S.; Rizzi, J.; Vieira, L.M.; Sanez, J. PAHs in Water, Sediment and Biota in an Area with Port Activities. *Arch Environ. Contam Toxicol.* **2018**, *75*, 236–246. [CrossRef]

7.   Solano, R.A.; De León, L.D.; De Ávila, G.; Herrera, A.P. Polycyclic aromatic hydrocarbons (PAHs) adsorption from aqueous solution using chitosan beads modified with thiourea, TiO2 and Fe3O4 nanoparticles. *Environ. Technol. Innov.* **2021**, *21*, 101378. [CrossRef]

8.   Gaurav, G.K.; Mehmood, T.; Kumar, M.; Cheng, L.; Sathishkumar, K.; Kumar, A.; Yadav, D. Review on polycyclic aromatic hydrocarbons (PAHs) migration from wastewater. *J. Contam. Hydrol.* **2021**, *236*, 103715. [CrossRef]

9.   Yang, R.; Zeng, G.; Xu, Z.; Zhou, Z.; Huang, J.; Fu, R.; Lyu, S. Comparison of naphthalene removal performance using H_2O_2, sodium percarbonate and calcium peroxide oxidants activated by ferrous ions and degradation mechanism. *Chemosphere* **2021**, *283*, 131209. [CrossRef]

10. Yang, R.; Zeng, G.; Xu, Z.; Zhou, Z.; Zhou, Z.; Ali, M.; Sun, Y.; Sun, X.; Huang, J.; Lyu, S. Insights into the role of nanoscale zero-valent iron in Fenton oxidation and its application in naphthalene degradation from water and slurry systems. *Water Environ. Res.* **2022**, *94*, e10710. [CrossRef]

11. Zhang, J.W.; Fan, S.S.; Lu, B.; Cai, Q.H.; Zhao, J.X.; Zang, S.Y. Photodegradation of naphthalene over Fe_3O_4 under visible light irradiation. *R. Soc. Open Sci.* **2019**, *6*, 181779. [CrossRef]

12. McQuillan, R.V.; Stevens, G.W.; Mumford, K.A. Assessment of the electro-Fenton pathway for the removal of naphthalene from contaminated waters in remote regions. *Sci. Total Environ.* **2021**, *762*, 143155. [CrossRef]

13. Zeng, G.; Yang, R.; Fu, X.; Zhou, Z.; Xu, Z.; Zhou, Z.; Qiu, Z.; Sui, Q.; Lyu, S. Naphthalene degradation in aqueous solution by Fe(II) activated persulfate coupled with citric acid. *Sep. Purif. Technol.* **2021**, *264*, 118441. [CrossRef]

14. Li, Y.H.; Zhao, L.; Chen, F.L.; Jin, K.S.; Fallgren, P.H.; Chen, L. Oxidation of nine petroleum hydrocarbon compounds by combined hydrogen peroxide/sodium persulfate catalyzed by siderite. *Environ. Sci. Pollut. Res.* **2020**, *27*, 25655–25663. [CrossRef]

15. Liang, C.; Guo, Y.-Y. Mass Transfer and Chemical Oxidation of Naphthalene Particles with Zerovalent Iron Activated Persulfate. *Environ. Sci. Technol.* **2010**, *44*, 8203–8208. [CrossRef]

16. Beninca, C.; Boni, E.C.; Goncalves, F.F.; Primel, E.G.; Freire, F.B.; Zanoelo, E.F. Photo-fenton and UV photo degradation of naphthalene with zero- and two-valent iron in the presence of persulfate. *Chem. Eng. Commun.* **2019**, *206*, 1–11. [CrossRef]

17. Sreeja, P.H.; Sosamony, K.J. A Comparative Study of Homogeneous and Heterogeneous Photo-fenton Process for Textile Wastewater Treatment. *Procedia Technol.* **2016**, *24*, 217–223. [CrossRef]

18. Shokri, A.; Fard, M.S. A critical review in Fenton-like approach for the removal of pollutants in the aqueous environment. *Environ. Chall.* **2022**, *7*, 100534. [CrossRef]

19. Lorenzo, D.; Santos, A.; Sánchez-Yepes, A.; Conte, L.Ó.; Domínguez, C.M. Abatement of 1,2,4-trichlorobencene by wet peroxide oxidation catalysed by goethite and enhanced by visible led light at neutral ph. *Catalysts* **2021**, *11*, 139. [CrossRef]

20. Vicente, F.; Rosas, J.M.; Santos, A.; Romero, A. Improvement soil remediation by using stabilizers and chelating agents in a Fenton-like process. *Chem. Eng. J.* **2011**, *172*, 689–697. [CrossRef]

21. Baciocchi, R. Principles, Developments and Design Criteria of In Situ Chemical Oxidation. *Water Air Soil Poll.* **2013**, *224*, 1717. [CrossRef]

22. Baciocchi, R.; D'Aprile, L.; Innocenti, I.; Massetti, F.; Verginelli, J. Development of technical guidelines for the application of in-situ chemical oxidation to groundwater remediation. *J. Clean. Prod.* **2014**, *77*, 47–55. [CrossRef]

23. Siegrist, R.L.; Crimi, M.; Simpkin, T.J. *In Situ Chemical Oxidation for Groundwater Remediation*; Springer: New York, NY, USA, 2011. [CrossRef]

24. Waclawek, S.; Lutze, H.V.; Grubel, K.; Padil, V.V.T.; Cernik, M.; Dionysiou, D.D. Chemistry of persulfates in water and wastewater treatment: A review. *Chem. Eng. J.* **2017**, *330*, 44–62. [CrossRef]

25. Tsitonaki, A.; Petri, B.; Crimi, M.; Mosbaek, H.; Siegrist, R.L.; Bjerg, P.L. In Situ Chemical Oxidation of Contaminated Soil and Groundwater Using Persulfate: A Review. *Crit. Rev. Environ. Sci. Technol.* **2010**, *40*, 55–91. [CrossRef]

26. Sra, K.S.; Thomson, N.R.; Barker, J.F. Stability of Activated Persulfate in the Presence of Aquifer Solids. *Soil Sediment. Contam.* **2014**, *23*, 820–837. [CrossRef]

27. Dahmani, M.A.; Huang, K.; Hoag, G.E. Sodium Persulfate Oxidation for the Remediation of Chlorinated Solvents (USEPA Superfund Innovative Technology Evaluation Program). *Water Air Soil Pollut. Focus* **2006**, *6*, 127–141. [CrossRef]

28. Rodriguez, S.; Santos, A.; Romero, A. Oxidation of priority and emerging pollutants with persulfate activated by iron: Effect of iron valence and particle size. *Chem. Eng. J.* **2017**, *318*, 197–205. [CrossRef]

29. Lominchar, M.A.; Santos, A.; de Miguel, E.; Romero, A. Remediation of aged diesel contaminated soil by alkaline activated persulfate. *Sci. Total Environ.* **2018**, *622*, 41–48. [CrossRef]

30. Liu, J.L.; Liu, Z.H.; Zhang, F.J.; Su, X.S.; Lyu, C. Thermally activated persulfate oxidation of NAPL chlorinated organic compounds: Effect of soil composition on oxidant demand in different soil-persulfate systems. *Water Sci. Technol.* **2017**, *75*, 1794–1803. [CrossRef]

31. Abdelhaleem, A.; Chu, W. Prediction of carbofuran degradation based on the hydroxyl radical's generation using the FeIII impregnated N doped-TiO_2/H_2O_2/visible LED photo-Fenton-like process. *Chem. Eng. J.* **2020**, *382*, 122930. [CrossRef]

32. Lorenzo, D.; Dominguez, C.M.; Romero, A.; Santos, A. Wet Peroxide Oxidation of Chlorobenzenes Catalyzed by Goethite and Promoted by Hydroxylamine. *Catalysts* **2019**, *19*, 553. [CrossRef]

33. Dominguez, C.M.; Romero, A.; Lorenzo, D.; Santos, A. Thermally activated persulfate for the chemical oxidation of chlorinated organic compounds in groundwater. *J. Environ. Manag.* **2020**, *261*, 110240. [CrossRef] [PubMed]

34. Huling, S.G.; Ko, S.; Park, S.; Kan, E. Persulfate oxidation of MTBE- and chloroform-spent granular activated carbon. *J. Hazard. Mater.* **2011**, *192*, 1484–1490. [CrossRef] [PubMed]

35. Hutson, A.; Ko, S.; Huling, S.G. Persulfate oxidation regeneration of granular activated carbon: Reversible impacts on sorption behavior. *Chemosphere* **2012**, *89*, 1218–1223. [CrossRef]

36. Kusic, H.; Peternel, I.; Ukic, S.; Koprivanac, N.; Bolanca, T.; Papic, S.; Bozic, A.L. Modeling of iron activated persulfate oxidation treating reactive azo dye in water matrix. *Chem. Eng. J.* **2011**, *172*, 109–121. [CrossRef]

37. Liang, C.; Wang, Z.S.; Mohanty, N. Influences of carbonate and chloride ions on persulfate oxidation of trichloroethylene at 20 degrees C. *Sci. Total Environ.* **2006**, *370*, 271–277. [CrossRef]